Hearing Research 430 (2023) 108721

Contents lists available at ScienceDirect

Hearing Research

journal homepage: www.elsevier.com/locate/heares

Human middle-ear muscle pulls change tympanic-membrane shape and low-frequency middle-ear transmission magnitudes and delays

Nam Hyun Cho[a,b], Michael E. Ravicz[a,b], Sunil Puria[a,b,c,*]

[a] Eaton-Peabody Laboratories, Massachusetts Eye and Ear, Boston, MA, USA
[b] Department of Otolaryngology, Harvard Medical School, Boston, MA, USA
[c] Graduate Program in Speech and Hearing Bioscience and Technology, Harvard University, Cambridge, MA, USA

ARTICLE INFO

Article history:
Received 5 August 2022
Revised 27 January 2023
Accepted 9 February 2023
Available online 11 February 2023

Keywords:
Middle ear
Tensor tympani muscle
Stapedius muscle
Sound transmission
Tympanic membrane
Middle-ear delay
Optical coherence tomography (OCT) vibrometry
Auditory and visual localization

ABSTRACT

The three-bone flexible ossicular chain in mammals may allow independent alterations of middle-ear (ME) sound transmission via its two attached muscles, for both acoustic and non-acoustic stimuli. The tensor tympani (TT) muscle, which has its insertion on the malleus neck, is thought to increase tension of the tympanic membrane (TM). The stapedius (St) muscle, which has its insertion on the stapes posterior crus, is known to stiffen the stapes annular ligament. We produced ME changes in human cadaveric temporal bones by statically pulling on the TT and St muscles. The 3D static TM shape and sound-induced umbo motions from 20 Hz to 10 kHz were measured with optical coherence tomography (OCT); stapes motion was measured using laser-Doppler vibrometry (LDV). TT pulls made the TM shape more conical and moved the umbo medially, while St pulls moved the umbo laterally. In response to sound below about 1 kHz, stapes-velocity magnitudes generally decreased by about 10 dB due to TT pulls and 5 dB due to St pulls. In the 250 to 500 Hz region, the group delay calculated from stapes-velocity phase showed a decrease in transmission delay of about 150 μs by TT pulls and 60 μs by St pulls. Our interpretation of these results is that ME-muscle activity may provide a way of mechanically changing interaural time- and level-difference cues. These effects could help the brain align head-centered auditory and ocular-centered visual representations of the environment.

1. Introduction

The middle ear (ME) of mammals conducts sound from the environment (via the ear canal) to the inner ear where the auditory sensory epithelium resides. The ME includes the tympanic membrane (TM) and an air-filled space (ME cavity) in which the ME bones (ossicles) reside. One of the well-established functions of the ME is to reduce the impedance mismatch between the low-density air lateral to the TM and the high-density fluid-filled inner ear (Møller, 1963).

The ME of mammals is unique among animals in that it contains three distinct ossicles, rather than one columella as found in birds, reptiles, and amphibians (e.g., Manley, 2010). In most mammals (including human, cat, and rabbit), these three ossicles (malleus, incus, stapes) have two joints between them and two muscles attached to them (Mason and Farr, 2013): the tensor tympani (TT) muscle attaches to the malleus neck, and the stapedius (St) muscle attaches to the stapes posterior crus just medial to the stapes head (Loeb, 1964; Mansour et al., 2013) – see Fig. 1 (Wang et al., 2006). Other components of the ME, such as the TM and ME air space, are found in other terrestrial vertebrate groups besides mammals (e.g., Tucker, 2017).

The functional and survival importance of the three-ossicle mammalian ME has been the topic of much speculation (e.g., Manley, 2010). The primary mode of motion of the ME ossicles – rotation around an axis approximately through the malleus and incus bodies – has been shown in some species to have a lower effective mass than the translational motion of a columella, which may aid in high-frequency hearing (Sim et al., 2007). Other suggested purposes of the ossicles and flexible joints include (a) protecting the inner ear from excessively high or low static pressures (Borg et al., 1984; Hüttenbrink, 1988b, 1992), (b) reducing the peak amplitudes of impulsive sounds reaching the cochlea by spreading their energy out over time (Gottlieb et al., 2018), and (c) enabling controlled alterations of ME sound transmission via the TT and St muscles (Marquet, 1981).

The St muscle is the smallest muscle in the human body and is densely innervated with motor neurons (Blevins, 1968). Much of what is known of its function comes from studies in animals

* Corresponding author at: Eaton-Peabody Laboratories, Massachusetts Eye and Ear, Boston, MA, USA.
E-mail address: sunil_puria@meei.harvard.edu (S. Puria).

https://doi.org/10.1016/j.heares.2023.108721
0378-5955/

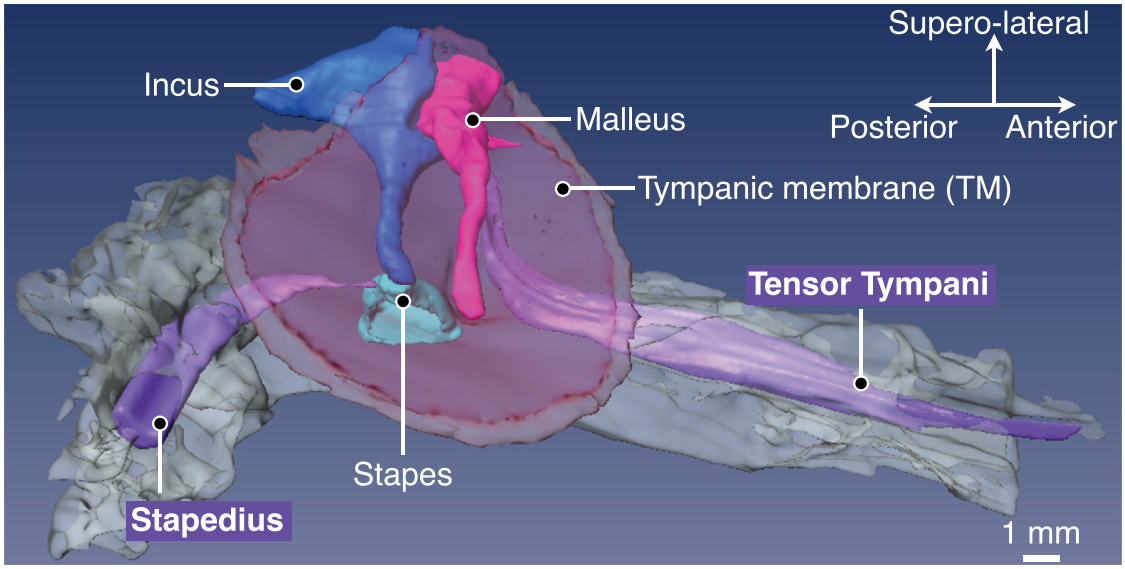

Fig. 1. A histology-based 3D reconstruction of a right ear (Wang et al., 2006) shows the anatomy of the human middle-ear (ME) structures (i.e., tympanic membrane [TM], malleus, incus, and stapes) with tensor tympani (TT) and stapedius (St) muscles (purple color). The bony tunnels (gray color) through which the TT (cochleariform process) and St muscles (pyramidal process) pass are lightly shaded to show the muscle bodies and connections to the malleus neck (TT) and posterior crus of the stapes (St), respectively.

(cat, rabbit, and guinea pig) in the 1970s (Bosatra et al., 1975; Nuttall, 1974; Teig, 1972a, 1972b). The St muscle is activated by high-level sound and is believed to be involved in the "acoustic reflex", which can protect the inner ear against steady-state high-intensity sound (Gelfand, 1998). St-muscle contraction reduces ME sound transmission by pulling the stapes head in a posterior direction, which is believed to increase the tension and thus the stiffness of the stapes annular ligament (Pang and Peake, 1986). Increasing the off-axis displacement of the stapes head causes additional reductions in ME sound transmission, which could reduce the upward spread of masking of high-frequency sound by low-frequency sound (Pang and Guinan, 1997).

Very little is known about the function of the TT muscle, and it has been questioned whether the TT has any function at all (Howell, 1984). Henceforth, we use "TT muscle" and "TT" interchangeably, and also for St. Both acoustic and non-acoustic events are thought to activate the TT muscle (reviewed in Gallagher et al., 2021). Some people can contract their TT voluntarily, which produces a visible change in the TM position or shape and is frequently accompanied by a perception of low-frequency rumble (Amoako-Tuffour et al., 2016; Fournier et al., 2022; Wickens et al., 2017). Applied TT tension in human cadaveric temporal bones produced tympanometric changes similar to those from voluntary TT contraction in human subjects (Aron et al., 2015). TT contraction is thought to increase tension of the TM, which could change the TM shape, and these effects are thought to modify ME transmission (Fay et al., 2006; Funnell and Laszlo, 1978). However, the effects of TT-muscle activity on TM shape and ME sound transmission are not well understood. Here we test a new hypothesis that ME-transmission phase, and thus delay, can be modulated via the ME muscles.

Middle-ear transmission is often quantified as stapes velocity normalized by ear-canal sound pressure, and we use this definition in this paper. ME-transmission delay is then defined in the frequency domain as the negative of the slope of the phase of the normalized stapes velocity. (In the time domain it is the interval between when an acoustic stimulus is presented in the ear canal and when the stapes responds to it.) In this paper, we use steady-state stimuli and evaluate ME delay in the frequency domain.

It has been shown that there is significant transmission delay through the ME. Puria and Allen (1998) showed that there is delay through the cat ME, which they attributed mostly to the TM but also to the ossicles. ME delays were also confirmed in gerbil (Olson, 1998) and human (O'Connor and Puria, 2006). In the cat and gerbil, the ME delay was estimated to be in the 25–40 μs range, while for human it was more than twice as long, approximately 40–160 μs. What role delays in the ME play in hearing is not known. In modeling studies, it was shown that ME delay increases the bandwidth of ME sound transmission (Parent and Allen, 2010; Puria, 2020; Puria and Allen, 1998). Finite-element modeling studies have suggested that a decrease in TM stiffness can increase the delay, while an increase in TM stiffness can decrease the delay by a factor of two, with the effect greatest for frequencies below about 1 kHz (O'Connor and Puria, 2006). This prompted us to look for the effects of ME-muscle tension at low frequencies, which had received little attention. In this paper we test a new hypothesis that another reason for ME delay is to provide a bias delay that can then be modulated via tension in the ME muscles.

An advantage to a bias delay in the ME is that it could be modulated in response to both acoustic and non-acoustic stimuli. Love and Stream (1978) argued that there is tonic muscle activity, which may provide a bias tension on the TM and stapes. Recent research documents ear-canal pressure changes coincident with eye saccades (Gruters et al., 2018). Several mechanisms were postulated, including ME-muscle modulation or the generation of otoacoustic emissions. In another study, voluntary unilateral eye closures coincided with ME-impedance changes (Tasko et al., 2022). If our hypothesis that ME-muscle pulls can modulate ME delay and attenuation is correct, particularly at low frequencies, then it would provide support for the idea that the ME muscles can modulate interaural localization cues and thus aid in sound localization, particularly in the horizontal plane.

This study explores the effects of TT and St muscle tension on several aspects of sound transmission (both magnitude and de-

lay) through the ME of human cadaveric temporal bones. We performed mechanically controlled pulls on the TT and St muscles at physiologically realistic levels and examined: (a) changes in velocity at the umbo ($\mathbf{V_U}$) – the ME input; (b) stapes velocity at the posterior crus ($\mathbf{V_S}$) – the middle-ear output and cochlear input; and (c) changes in TM shape and umbo displacement due to static ME muscle pulls. TM shape was measured using 3D volumetric optical coherence tomography (OCT). This study extends earlier work by Love and Stream (1978) and Hüttenbrink (1988b) to quantify how TT or St muscle pulls affect ME sound transmission and TM shape changes in human. We explore the consequences of ME muscle pulls, particularly below 1 kHz, and the impact they may have on sound localization.

2. Materials and methods

2.1. Human temporal-bone preparation

Four freshly frozen unfixed human adult temporal bones (TB11, TB13, TB14, TB15), obtained from Anatomy Gifts Registry (Hanover, MD), were used in this study. All four specimens were from donors with no otologic disease history, and we confirmed that all specimens were free of ME pathologies by visual examination before drilling and after beginning preparation. TB11: female, 56 years old at death, right ear; TB13: male, 68 years old, left ear; TB14: male, 63 years old, left ear; TB15: same donor as TB13, right ear. A plug about 8 cm on a side was cut from the temporal bone and stripped of the skin and pinna at the time of harvest, preserving the external ear canal and all middle- and inner-ear structures. TB11 was used to develop technique. The procurement and use of the temporal bones was in accordance with the Institutional Review Board (IRB) of Massachusetts Eye and Ear.

The temporal bones were thawed in 0.9% normal saline for 10 min before preparation. The bony ear canal was carefully drilled away to completely expose the lateral side of the TM. The ME cavity and facial recess were opened for access to the stapes posterior crus and St muscle (similar to Hüttenbrink, 1988b) and remained open during measurements. A hole was drilled anterior to the TM for access to the TT muscle body. The TT and St muscles were detached from their bony anchors at the proximal end. The bony tunnels through which the TT and St pass (TT: cochleariform process; St: pyramidal process) were preserved so that pulling on the TT or St would produce a force on the malleus or stapes, respectively, in the anatomically correct direction (Figs. 1 and 2).

For measurements, the temporal bone was fixed with dental cement (Durelon^{TM}, 3 M ESPE SA, Germany) to a metal post that was clamped in a one-axis micro-positioner mounted on an X-Y-rotary table to allow the temporal bone to be oriented with the tympanic ring approximately orthogonal to the vertical optical axis of the OCT system. During experiments, the temporal bone was kept moist by saline-moistened gauze. For TB14 and TB15, a water mist was applied with a humidifier between measurements to keep the specimens moist.

2.2. Pulling on the middle-ear muscles

To apply known amounts of pull to the TT and St muscles, locking forceps mounted on a force sensor (SMD2387–02–002 or –010; Strain Measurement Devices, Wallingford, CT, USA) grasped each muscle body near its bony tunnel (Fig. 2). By preserving the bony tunnels, we ensured that the muscle pull was applied through the tendon to its anchor on the ossicle in its natural direction. We had no way to account for friction between the tendon and the tunnel wall (e.g., Hüttenbrink, 1988b), so we tried to minimize its effects by keeping the ME and TM moist and applying pulls at the muscle body. The force sensors were mounted on 3-axis micromanipulators for control of force with ±5 mN precision. The force sensors were calibrated in their orientation during use with 4–7 weights spanning the range of pulls. The weights were suspended by strings routed over rods to deliver the force to the force sensor in the same direction as the muscle pull, and the calibration was computed from the slope of the force–output curve to minimize the effect of friction between the strings and the rod.

As the forces exerted by the human ME muscles are not known, to estimate reasonable forces to apply in human temporal bones, we started with the reported average forces produced by ME muscles under steady pulsatile electrical stimulation in live cats and rabbits (Teig, 1972a): TT forces: 530 mN in cat, 320 mN in rabbit; St forces: 135 mN in cat, 150 mN in rabbit. Previous estimates of human TT and St force in the literature (reviewed in Hüttenbrink, 1988a) range to 500 mN for TT and 150 mN for St. (Hüttenbrink, 1988b used lower forces in static-displacement experiments: 100 mN for TT, 50 mN for St.) An allometric analysis (Rosowski, 1994) has shown that the TM and stapes-footplate areas vary with the ¼ power of animal body weight, which suggests that the cross-sectional area of the TT and St in human (body weight 30–40x cat or rabbit; Rosowski, 1994) should be larger by about a factor of ~2.5. Assuming that muscle force varies in proportion to the cross-sectional area of the muscle, forces roughly twice those of cat or rabbit are likely to be in the physiological range for human. From this analysis, we estimate the maximum TT force in live human to be about 1000 mN and the maximum St force to be about 300 mN.

During the measurements, we began with small forces (50–100 mN) and then increased the force as much as practicable. The maximum St forces applied (up to 800 mN) are approximately 3x those estimated for the human St muscle; the TT forces we could apply (typically up to ~500 mN and ~1 N in one temporal bone) were limited by our ability to grasp the TT muscle in these bones and were within the maximum estimated for the human TT muscle.

Muscle tension decreased during a measurement, due to viscoelastic relaxation of the muscle tissue. For each muscle-pull measurement, the micromanipulator with the forceps and force sensor was moved until the resulting muscle force was ~10% higher than desired. The force decreased with time but remained within approximately 5% of the reported nominal value during the measurements.

Stapedius forces ranged from 0 to approximately 800 mN in several steps, while TT forces ranged from 0 to approximately 500 mN in several steps. Higher-pull-force measurements (in which damage would be more likely to occur; Lauxmann et al., 2012) were performed near the end of experiments. Zero-mN-pull baseline umbo and stapes-velocity measurements were performed before muscle pulls, after every few measurements with muscle pulls, and at the end of muscle-pull measurements. Similarly, umbo displacement with zero pull (the “rest state”) was measured before and after displacement with muscle pulls. Only those measurements for which baseline measurements before and after differed by less than 20% (~2 dB) are included in the reported data.

2.3. Stimulus sound generation and measurement

The TM and ME were stimulated by a series of pure tones generated by LabVIEW-based (NI, Austin, TX, USA) custom software (SyncAv version 0.34) running on a PC with a National Instruments PCI-4461 board and delivered through a Beyerdynamic DT-48 earphone (Heilbronn, Germany). A series of 59 tones between 23.4 Hz and 10 kHz with logarithmic spacing was conducted to an ear-canal coupler via a flexible rubber tube to reduce vibrations transmitted from the earphone. A probe tube attached to a microphone (EK23103; Knowles, Itasca, IL) was introduced through a hole in

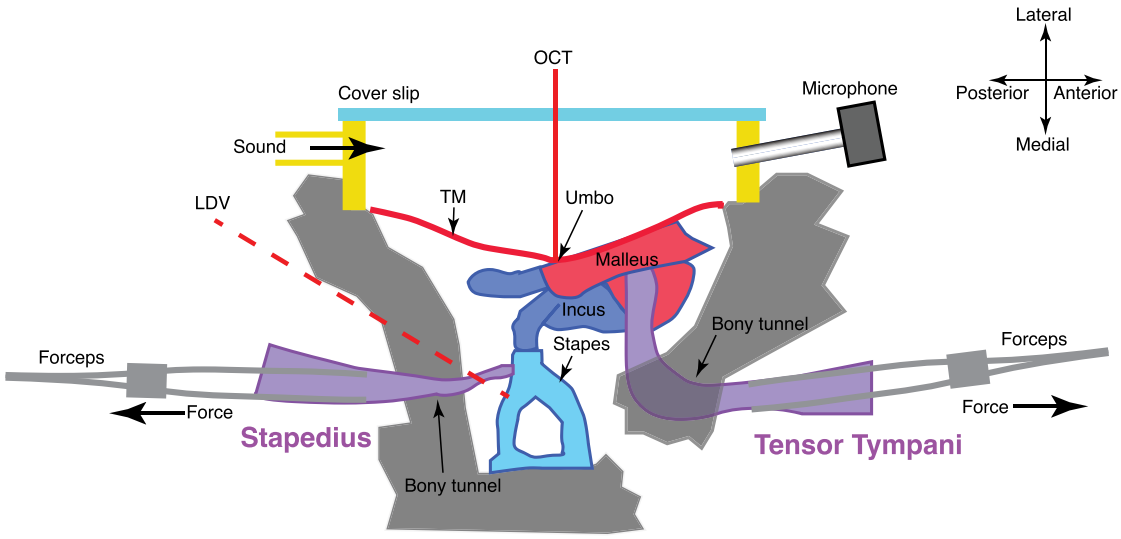

Fig. 2. Schematic diagram of the experimental setup. Velocity of the TM above the umbo (V_U) in response to sound was measured with optical coherence tomography (OCT) vibrometry (both magnitude and phase) by shining the beam through the cover slip that acoustically sealed the ear canal. Stapes velocity (V_S) was measured simultaneously on the stapes posterior crus with laser Doppler vibrometry (LDV). Ear-canal sound pressure (P_{EC}) was measured with a microphone located near the edge of the TM. A pull was applied to the TT or St muscle by grasping the muscle body with locking forceps attached to a force sensor and micromanipulator (not shown). The bony tunnels through which the TT and St muscles pass were preserved to ensure that force was applied to the malleus or stapes in its anatomically appropriate direction. For shape measurements, the cover slip was not present, and volumetric OCT measured the shape of the entire TM from several image acquisitions spanning the depth of the TM.

the coupler and positioned within about 2–3 mm of the TM near the edge to measure ear-canal pressure ($\mathbf{P_{EC}}$). $\mathbf{P_{EC}}$ responses were recorded by the SyncAv software. The measured microphone response was then used to vary the stimulus voltage to produce a nearly constant $\mathbf{P_{EC}}$ of 94–100 dB SPL across frequencies (Cho and Puria, 2022). The ear-canal coupler had a glass back (cover slip) to allow visual access to nearly the entire TM for the OCT system to measure TM velocity near the center of the umbo (see Fig. 2).

2.4. Umbo- and stapes-velocity measurements

The velocity of the TM at the umbo $\mathbf{V_U}$ and stapes velocity $\mathbf{V_S}$ were measured simultaneously with $\mathbf{P_{EC}}$. $\mathbf{V_U}$ was measured through the glass-backed EC coupler with the OCT system and custom VibOCT software as described below, at a single location approximately above the center of the umbo. $\mathbf{V_S}$ was measured at a single point on a small (∼0.5 mm square) retroreflective target on the stapes posterior crus near the stapes head with a laser-Doppler vibrometer (LDV; CLV-1000, Polytec, Waldbronn, Germany). The angle between the measurement direction and the stapes piston direction was approximately 45°, and this angle did not change appreciably during St pulls. $\mathbf{V_S}$ responses and $\mathbf{P_{EC}}$ were recorded by the SyncAv software. All reported velocity measurements were normalized by $\mathbf{P_{EC}}$.

2.5. Optical coherence tomography (OCT) system for TM shape and vibrometry

All OCT imaging and vibrometry data were acquired using a Ganymede-III-HR 905-nm OCT system (Thorlabs, Germany) with a high-speed (up to 100-kHz frame rate) line-scan camera. The OCT system was operated using custom LabVIEW-based VibOCT software (version 1.6), which measured TM velocity at a single location as well as the 3D shape of the TM without and with muscle pulls. The axial resolution was ∼2.7 μm (in air), and the lateral resolution with a 36-mm, 0.055-NA, 2 × objective lens (OCT- LK3-BB, Thorlabs) was ∼18 μm. Details about our OCT system and related methodology have been reported previously (Cho et al., 2022; Cho and Puria, 2022).

2.5.1. OCT vibrometry

For OCT vibrometry, velocity acquisition at 1024 depths simultaneously along a single vertical track (A-line) was synchronized with the tone stimuli by an external trigger provided by the SyncAv software. TM velocity was evaluated at the TM surface at the umbo. The system was calibrated against the LDV on an electrodynamic minishaker or piezoelectric speaker. The system's dynamic range was at least 80 dB over the 0.1–24 kHz frequency range. In general, the system noise floor was ∼1 nm at 0.1 kHz and decreased to below 0.1 nm from ∼8 kHz up to 24 kHz.

2.5.2. Volume imaging for TM shape

For 3D OCT imaging of the TM, we acquired 8–10 overlapping 3D volume scans (C-scans) at successively medial focal depths by moving the optical head vertically downward toward the TM, as the penetration depth of our OCT system (∼1.91 mm in air) and depth range of best image quality (< 0.4 mm) are less than the depth of most human TMs (∼1.5–2.5 mm). The maximum transverse scanning range was 10 mm, which covers the human TM diameter. A single 3D C-scan consisted of a longitudinal stack of 512 2D B-scans; each B-scan comprised 512 transverse A-lines of 1024 vertical points. Each 3D volume scan was an average of 10 C-scans. (See Cho et al., 2022 for more details.) No sound stimulus was presented during the volume scans. To acquire the C-scans necessary to measure the entire TM shape took ∼5–6 min.

A volume scan of the entire TM was constructed from the individual 3D volumes using the FIJI package of the public image processing program ImageJ (ImageJ.nih.gov). Each 3D volume was rotated as necessary and resliced to produce a vertical stack of horizontal sections approximately parallel to the tympanic ring. A portion of the vertical range of the best image ("best volume") was extracted from each 3D volume. These "best volumes" were concatenated to obtain a 3D volume image of the entire TM, as described previously for the cochlea (Cho et al., 2022).

A volume rendering of the 3D TM shape was performed using Amira (Thermo Fisher Scientific; Waltham, MA, USA). TM profiles were digitized from sections of the 3D TM shape and loaded into MATLAB (MathWorks, Natick, MA, USA) for further analysis.

2.6. Validity and stability of measurements

Measured velocities were generally stable throughout the experiment, as long as the temporal bone was kept moist. The glass-backed coupler helped to keep the TM moist. For TB14 and TB15 we implemented the humidification regime to maintain moistness of the ME. We then examined the effects on $\mathbf{V_U}$ and $\mathbf{V_S}$ of allowing TB15 to dry. The effect of drying (~2 dB over 2 h) was smaller than the effect of the smallest ME muscle pulls we applied.

As described in Section 2.2 above, zero-pull baseline measurements were made at the beginning of a measurement session and repeated after every 2–3 muscle pulls (up to 15 times for TT pulls, and up to 7 times for St pulls, depending on the bone). If the baseline measurement after a series of 2–3 pulls did not match the baseline before the pulls within ~20% (~2 dB), the muscle-pull measurements were repeated. Figs. 4 and 6 show that, for TT and St pulls in TB15, the standard error of the mean (s.e.m.) of zero-pull $\mathbf{V_U}$ and $\mathbf{V_S}$ measurements was generally less than ±1 dB over the entire frequency range, indicating that the baseline state of the temporal bone was nearly constant during the measurement series and that any drying effects were minimal. This also indicates that muscle pulls did not damage or alter the normal ME.

The open ME may have provided less opposition to TM movement by muscle pulls than an intact ME cavity, and the sealed ear canal may have provided more opposition to TM movement than an open ear canal. These effects are small and would tend to cancel. Even the largest umbo displacement we observed (~0.2 mm) would cause a change in ear-canal or ME volume of less than 1%, so the effects of the open ME and closed ear canal are likely not significant.

3. Results

In these specimens, $\mathbf{V_S}$ measurements normalized by $\mathbf{P_{EC}}$ fell within the normal range described in ASTM F2504–05 (Rosowski et al., 2007). While we present detailed results from one representative temporal bone (TB15), similar results were observed in the other bones (TB13 and TB14). Muscle-pull forces in TB11 were not quantified, but the results were qualitatively similar to those obtained in the other bones. The summary figure in the Discussion Section (Fig. 11) contains all valid velocity data.

3.1. Effects of ME muscle pulls on umbo and stapes velocities

3.1.1. Umbo and stapes velocities with no muscle pull

With no force applied to the TT and St muscles, both $\mathbf{V_U}$ and $\mathbf{V_S}$ were typical of what we and others have seen in the past (Fig. 3, black lines). $\mathbf{V_U}$ magnitude was higher than $\mathbf{V_S}$ magnitude (denoted by $|\mathbf{V_U}|$ and $|\mathbf{V_S}|$, respectively; top panels) at all frequencies, as has been seen previously. Attaching the forceps had virtually no effect on $\mathbf{V_U}$ or $\mathbf{V_S}$. At low frequencies (below about 0.7 kHz), $|\mathbf{V_U}|$ and $|\mathbf{V_S}|$ increased proportionally with frequency, and the phases (denoted by $\angle\mathbf{V_U}$ and $\angle\mathbf{V_S}$, respectively; bottom panels) were between +0.125 and +0.25 cycles. The magnitude and phase are internally consistent and indicate that the middle ear is a stiffness-controlled system at low frequencies.

Around 1–3 kHz, $|\mathbf{V_U}|$ and $|\mathbf{V_S}|$ reach a maximum and the phases cross 0 cycles. At higher frequencies, $|\mathbf{V_U}|$ and $|\mathbf{V_S}|$ decrease, but much less than proportionally to frequency, and $\angle\mathbf{V_U}$ and $\angle\mathbf{V_S}$ continue to accumulate beyond –0.25 cycles, which is indicative of delay in the system.

3.1.2. Tensor-tympani muscle pulls

With various pull forces applied to the TT muscle, both $\mathbf{V_U}$ and $\mathbf{V_S}$ were affected (see Fig. 3): $|\mathbf{V_U}|$ and $|\mathbf{V_S}|$ (top panels) were reduced monotonically and approximately uniformly below about 1.5 kHz as the TT pull force was increased from 0 to 380 mN in several steps. The effect was relatively larger on $\mathbf{V_S}$ (panel B) than on $\mathbf{V_U}$ (panel A). $\angle\mathbf{V_U}$ and $\angle\mathbf{V_S}$ (bottom panels) also showed similar effects: The phases increased monotonically (the slope became less negative) with pull below about 2 kHz. At higher frequencies, TT pulls had little effect on $\mathbf{V_U}$ and a complicated effect on $\mathbf{V_S}$. At low frequencies $|\mathbf{V_U}|$ and $|\mathbf{V_S}|$ increased proportionally with frequency, and $\angle\mathbf{V_U}$ and $\angle\mathbf{V_S}$ were between 0 and +0.25 cycles, which is an indication that the ME continued to be stiffness dominated and that the stiffness increased with increasing muscle pulls.

The effects of TT pulls on $\mathbf{V_U}$ and $\mathbf{V_S}$ magnitudes can be seen more clearly when normalized by the zero-pull-case baseline (Fig. 4). Increasing TT pulls reduced $|\mathbf{V_U}|$ and $|\mathbf{V_S}|$ by increasing amounts roughly uniformly with frequency below about 1 kHz. Above 1.5 kHz, changes in $|\mathbf{V_U}|$ were small, occurred in small frequency ranges (~1/2 octave), and were roughly independent of pull force, while changes in $|\mathbf{V_S}|$, though also similar in small frequency ranges, were larger than the $|\mathbf{V_U}|$ changes. Even for the smallest TT pulls, changes in $|\mathbf{V_U}|$ and $|\mathbf{V_S}|$ were substantially larger than the variability in the zero-mN-pull baseline measurements (shaded region = s.e.m) at nearly all frequencies.

3.1.3. Stapedius muscle pulls

Fig. 5 shows $\mathbf{V_U}$ and $\mathbf{V_S}$ with pulls of various forces (up to 780 mN) applied to the St muscle. As for the case with TT pulls, the effects of St pulls on $|\mathbf{V_U}|$ and $|\mathbf{V_S}|$ (Fig. 5A, B) and phases (Fig. 5C, D) occurred primarily at low frequencies (below about 1 kHz) and were monotonic with pull force. At these low frequencies, the effect of St pull was greater on $\mathbf{V_S}$ than on $\mathbf{V_U}$. The effects on $|\mathbf{V_S}|$ were qualitatively similar but smaller than those seen by Pang and Peake (1986) with unknown forces in cat. Between 0.8 and 2 kHz, the effect on $|\mathbf{V_U}|$ was opposite to that at lower frequencies. Above 2 kHz there was virtually no effect on $\mathbf{V_U}$ and $\mathbf{V_S}$ due to St pull.

As with TT pulls in Fig. 4, the effects of St pulls on $\mathbf{V_U}$ and $\mathbf{V_S}$ magnitudes can be seen more clearly when normalized by the zero-pull-case baseline (Fig. 6). Increasing St pulls reduced $|\mathbf{V_U}|$ and $|\mathbf{V_S}|$ roughly uniformly with frequency below about 1 kHz and increased $|\mathbf{V_U}|$ between 1 and 2 kHz. At higher frequencies, St pulls had little effect on $|\mathbf{V_U}|$ or $|\mathbf{V_S}|$. In comparison to TT pulls (Fig. 4), the effect of St pulls was significantly smaller in magnitude, even though the St pull forces were nearly twice as large. As for TT pulls, changes in $|\mathbf{V_U}|$ and $|\mathbf{V_S}|$ were substantially larger than the s.e.m. of the zero-mN-pull baselines (shaded region) at nearly all frequencies.

3.1.4. ME-muscle-pull effects on the umbo- and stapes-velocity group delays

To quantify the effects of TT and St pulls on $\mathbf{V_U}$ and $\mathbf{V_S}$ phases, we observed that the slopes of $\angle\mathbf{V_U}$ and $\angle\mathbf{V_S}$ with frequency (when plotted on a linear frequency scale) were approximately constant in a low-frequency range in which the effects of TT or St pulls on velocity magnitudes (Fig. 4 or 6, respectively) were approximately constant. Fig. 7 shows an example in TB15 of how a line was fit to each $\angle\mathbf{V_S}$ curve in the 250–500 Hz range for the various TT (Fig. 7A) and St (Fig. 7B) pulls (minimum-mean-squared error fit). The negative of the slope of this fitted line with frequency is the group delay over this frequency range. Fig. 7 shows that the $\angle\mathbf{V_S}$ slope became less negative with increasing muscle pull: the group delay decreased from about 185 μs for the no-pull baseline to about 73 μs for a maximum TT-muscle pull of 380 mN, and from 170 μs for the no-pull baseline to about 53 μs for a maximum St-muscle pull of 780 mN. (Note that the baseline $\mathbf{V_S}$ group delays are slightly different for TT and St pulls, as these measurements were performed on different days.)

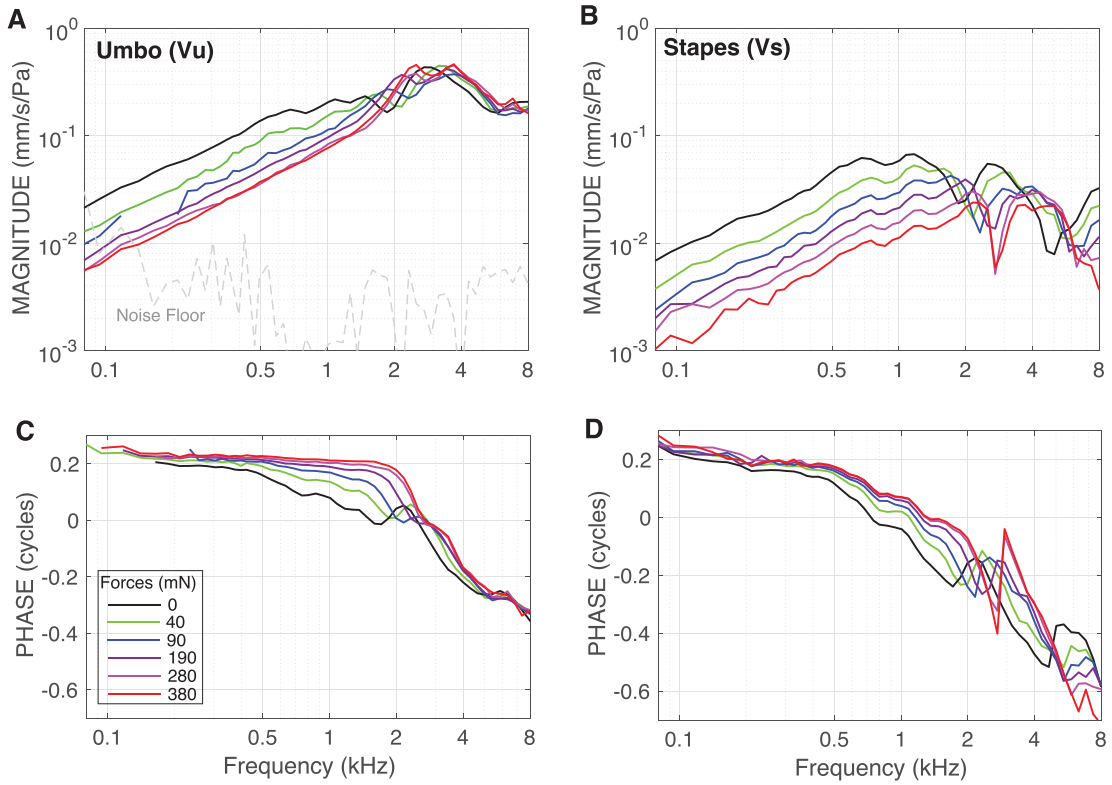

Fig. 3. V_U and V_S with various TT-muscle pulls and a baseline zero-mN-pull measurement, normalized by P_{EC}. (A–B) V_U and V_S magnitude normalized by P_{EC} (in units of [mm/s]/Pa). (C–D) V_U and V_S phase (in cycles), respectively. See legend in C for TT pull forces (in millinewtons). Specimen TB15.

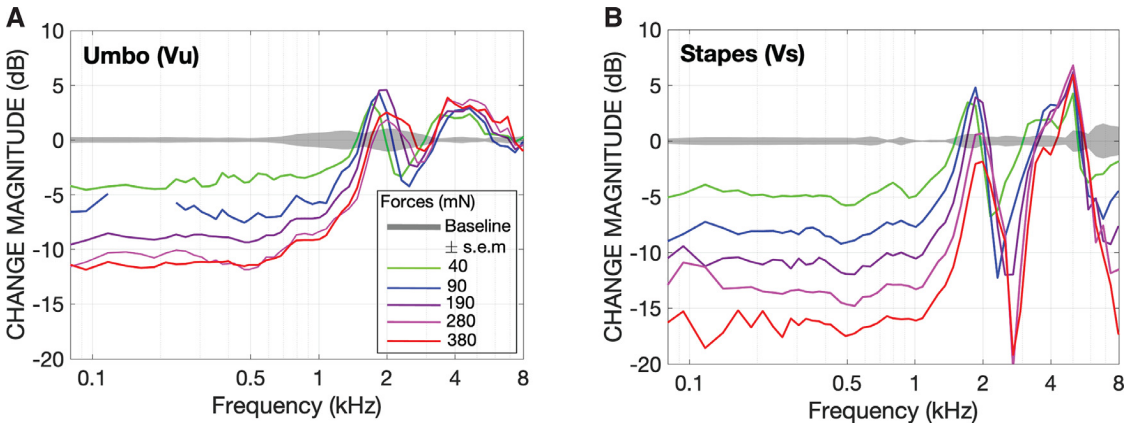

Fig. 4. Change in V_U (A) and V_S (B) magnitudes due to various TT pulls (see legend in A), relative to the mean of all valid zero-pull baseline measurements. The ± standard error of the mean (s.e.m.) of all baseline TT-pull measurements (in this temporal bone, $n = 15$) is shown as the gray shaded region. TB15.

3.1.5. Summary of ME-muscle-pull effects on V_U and V_S

The low-frequency effects of TT and St pulls on $\mathbf{V_U}$ and $\mathbf{V_S}$ magnitudes and group delays in measurements from all temporal bones ($n = 3$) are summarized in Fig. 8. The magnitude changes and group delays were evaluated over the 250–500 Hz range in TB13 and TB15 and a slightly higher frequency range (550–800 Hz) in TB14 to avoid low-frequency noise (muscle-pull effects on $|\mathbf{V_U}|$ and $|\mathbf{V_S}|$ in this range were still approximately constant with frequency). In all bones, TT-muscle pulls reduced $|\mathbf{V_U}|$ and $|\mathbf{V_S}|$ generally monotonically with increases in pull force (Fig. 8A). The effects on $|\mathbf{V_S}|$ were slightly larger than the effects on $|\mathbf{V_U}|$, but the effects on both had the same profile with pull force. In all bones, the reductions in $|\mathbf{V_U}|$ and $|\mathbf{V_S}|$ (in dB) with pull could be fit with a straight line for low pull forces (below ~300 mN), which suggests an exponential relationship between velocity reduction and pull force. Above this low-pull range, TT-muscle-pull effects began to saturate, and disproportionally higher pull forces were needed to produce an additional reduction in $|\mathbf{V_U}|$ or $|\mathbf{V_S}|$.

In all temporal bones with valid measurements, St pulls also reduced $\mathbf{V_U}$ and $\mathbf{V_S}$ magnitudes generally monotonically with increasing pull forces (Fig. 8B). The effects on $|\mathbf{V_S}|$ were larger than the effects on $|\mathbf{V_U}|$, but the effects on both had the same profile with pull force. The effects of St pulls on $|\mathbf{V_U}|$ and $|\mathbf{V_S}|$ were smaller than the effects of TT pulls.

Fig. 8C–D show the effects of TT and St pulls on low-frequency group delays. In all temporal bones, TT pulls reduced $\mathbf{V_U}$ and $\mathbf{V_S}$ delays generally monotonically with increases in pull force (Fig. 8C). The effects of TT pulls on $\mathbf{V_U}$ delays were generally

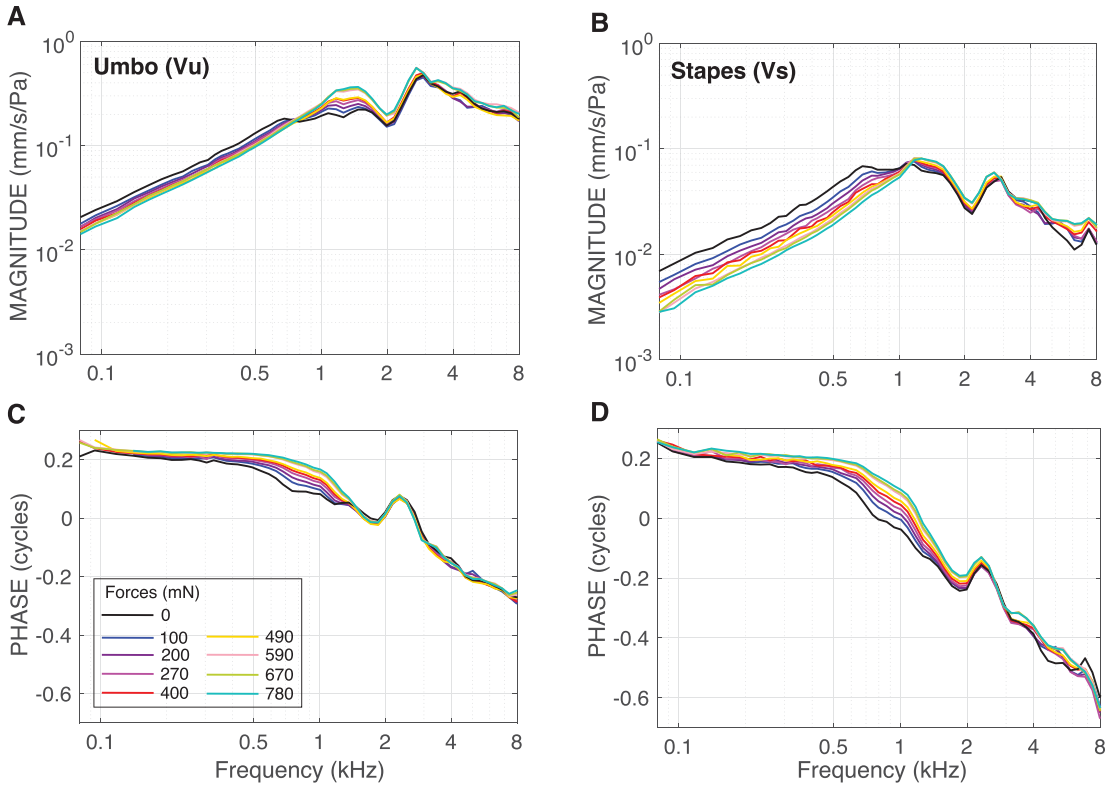

Fig. 5. V_U and V_S with various St-muscle pulls and a baseline zero-mN-pull measurement (normalized by P_{EC}). (A–B) $|V_U|$ and $|V_S|$; (C–D) $\angle V_U$ and $\angle V_S$, respectively. See legend in C for St pull forces. TB15.

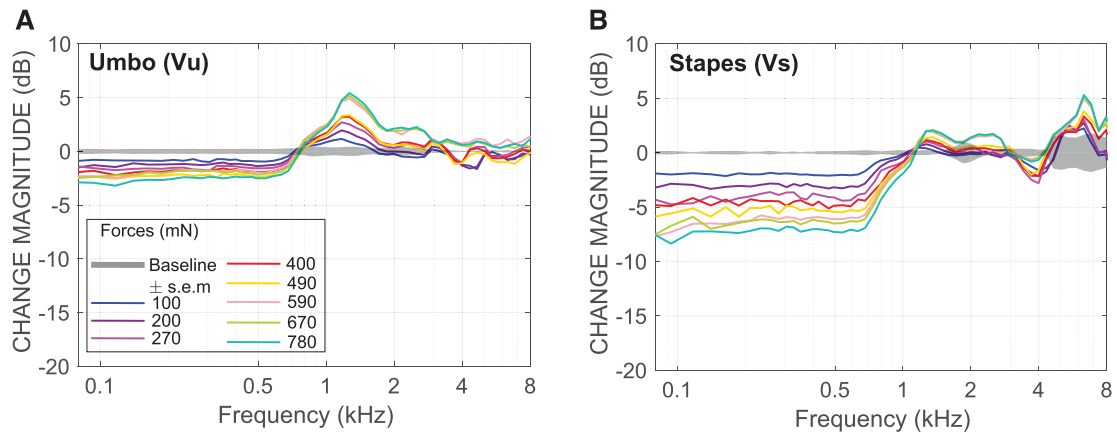

Fig. 6. Change in V_U (A) and V_S (B) magnitudes due to various St pulls (see legend in A, normalized by the mean of all valid baseline measurements. The ± standard error of the mean (s.e.m.) of all baseline muscle-pull measurements ($n = 7$ for St pulls in this temporal bone) is shown as the gray shaded region. TB15.

slightly larger than on $\mathbf{V_S}$ delays, but the effects on both generally had the same profile with pull force. The reductions in $\mathbf{V_U}$ and $\mathbf{V_S}$ delays were approximately linear with pull for low pull forces (<150–300 mN). Above this linear range (over ~300 mN), a much higher pull force was needed to produce an additional reduction in $\mathbf{V_U}$ or $\mathbf{V_S}$ delay, indicating saturation.

The effects of St pulls on group delays were also approximately monotonic with pull force and seemed to be approximately linear at low pull forces (Fig. 8D). St pulls produced similar or smaller reductions in $\mathbf{V_U}$ and $\mathbf{V_S}$ group delays in TB15 than TT pulls did (Fig. 8C). $\mathbf{V_U}$ phase data in TB14 were noisy at low frequencies, and the group delay could not be estimated reliably, so they are omitted from Fig. 8D. These results are further summarized in the linear pull-response range in the Discussion in Section 4 below.

3.2. TM shape change with ME muscle pulls

To understand how the ME muscles affect the TM shape, a 3D volume image of the entire TM in each temporal bone was constructed from concatenated OCT volume scans as described in the Methods (Section 2.5.2). Fig. 9 shows the 3D volume image of the TM in TB15 in its rest state and with various pulls. The posterior–anterior and inferior–superior profiles (along the lateral surface) in the three temporal bones are similar to previous results (Khaleghi et al., 2016; Van der Jeught et al., 2013). The normal shape of the TM has been described as having an inner conical section near the umbo (axial curvature only; the radial profile is approximately a straight line) and an outer toroidal section (with

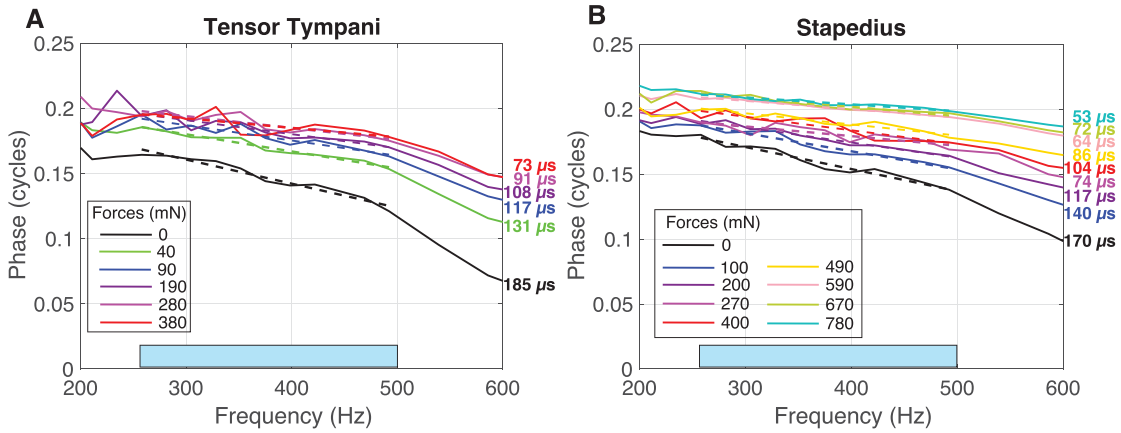

Fig. 7. Velocity group delay was computed from the velocity phase by fitting a straight line (dashed lines) to the phase (when plotted on a linear frequency scale) and computing the slope with respect to frequency. This example shows $\angle V_S$ in TB15 over the 250–500 Hz frequency range (colored bar at the bottom) with various TT (A) and St (B) pulls. A straight line (dashed) was fit to $\angle V_S$ in the low-frequency range where the magnitude change was constant with frequency – see Fig. 4B and Fig. 6B, respectively. The computed group delay for each muscle pull is shown by the label next to each colored line.

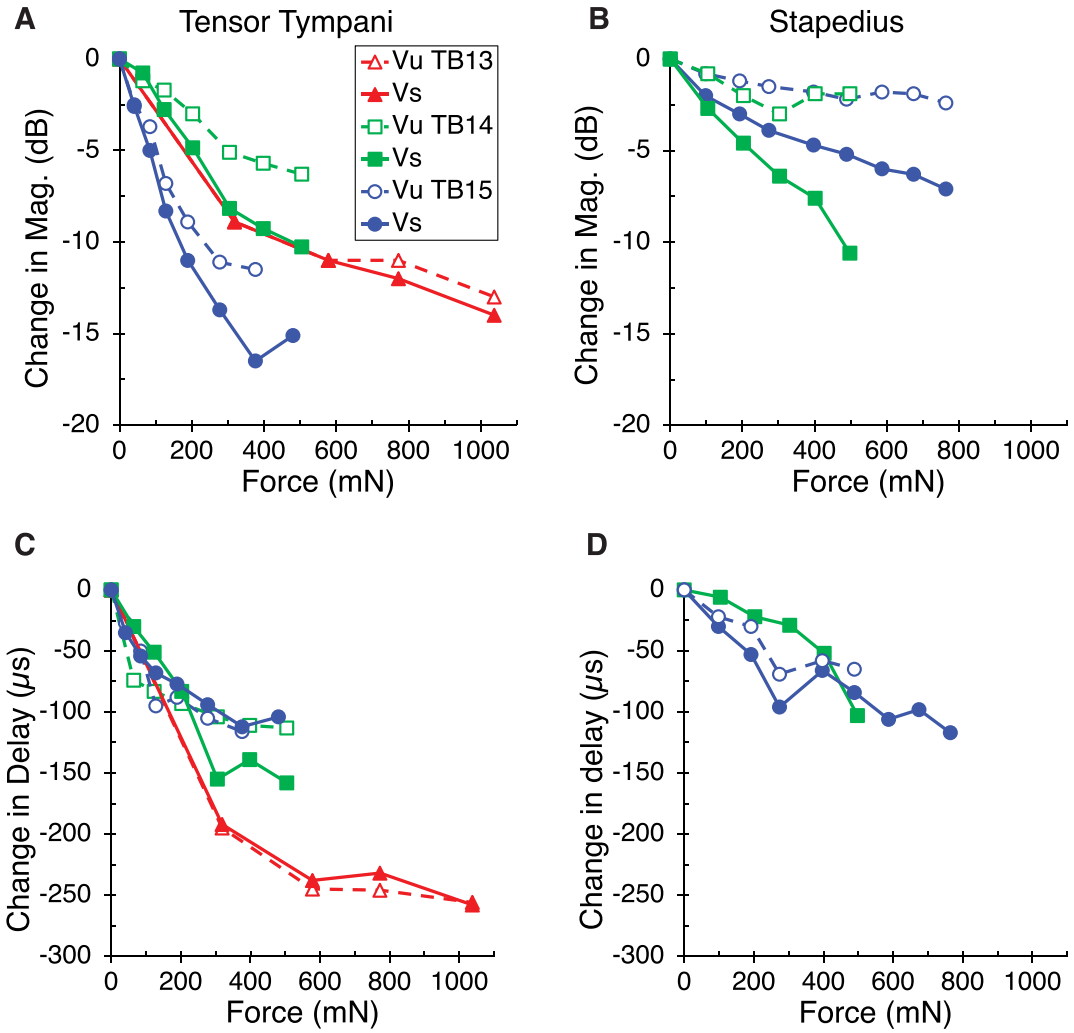

Fig. 8. Summary of low-frequency TT- and St-muscle-pull effects on representative V_U and V_S measurements in all three temporal bones (TB13, TB14, TB15), evaluated over a frequency range within 250–500 or 550–800 Hz, depending on the bone (see text). (A–B) Change in $|V_U|$ and $|V_S|$ (in dB) by (A) TT or (B) St pulls. (C–D) Change in V_U and V_S group delay (in μs) by (C) TT or (D) St pulls. V_U: open symbols and dashed lines; V_S: closed symbols and solid lines; TB13: red triangles; TB14: green squares; TB15: blue circles (see legend in A). No valid St-pull data were available for TB13, nor valid V_U delay data for TB14 with St pulls.

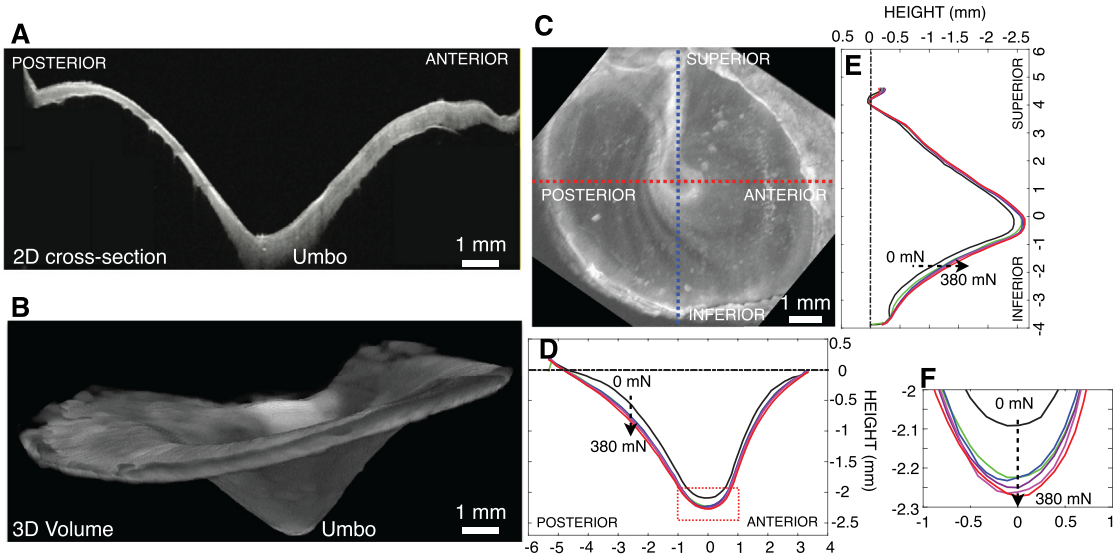

Fig. 9. TM shape change and umbo displacement due to TT-muscle pulls in TB15. (A) Cross section of the 3D volume image in (B) along a posterior–anterior TM diameter. (B) Reconstructed 3D volume image of the entire TM in its rest state (no muscle pull), generated by concatenating OCT volumes acquired at successive focal depths. (C) en-face view of the TM looking medially, showing posterior–anterior and inferior–superior diameters for shape evaluation. (D–E) Extracted shape profiles of the lateral TM surface (D) from posterior to anterior (red dotted line in C) and (E) superior to inferior (blue dotted line in C) directions, with the plane of the tympanic ring set to 0. The black curve is the profile in the rest state (0 mN); colored curves show the profile with increasing TT pulls to 380 mN (same color code as in Figs. 3 and 4). (F) Enlarged view of the umbo region in the red dotted rectangle in (D) showing umbo displacement in more detail.

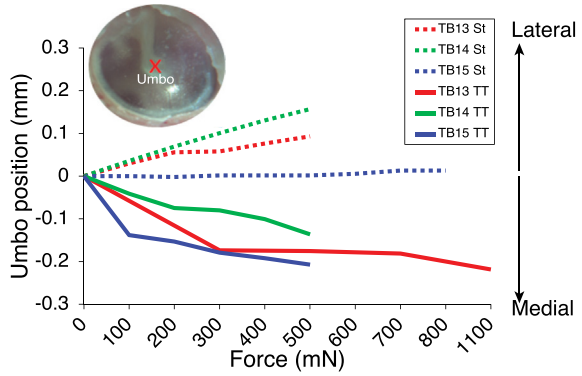

Fig. 10. Umbo position changes by example static TT and St pulls (solid and dotted lines, respectively) in all temporal bones: TB13 (red), TB14 (green), TB15 (blue). The inset photograph (recorded by the OCT video camera) indicates the displacement-evaluation location at the umbo (red ×).

both axial and radial curvature; Fay et al., 2006) – see Fig. 9A, B, D.

Fig. 9D–F show extracted TM shape profiles (in the posterior–anterior and inferior–superior directions, respectively) in TB15 with various TT pulls. St pulls had very little effect on TM shape, and are not shown (but see Fig. 10). As the TT pull increased to 380 mN, the umbo was displaced medially (panel F), and the shape of the TM in these regions flattened out as the portion of the TM in the middle of the span between the umbo and the tympanic ring moved medially with the toroidal region becoming more conical (panels D, E).

Fig. 9F indicates that the initial pull of 100 mN displaced the umbo medially by ~120 μm, and additional pulls produced only small increases in umbo displacement. When the TT muscle was pulled, the manubrium rotated slightly about the malleus lateral process (Panel E) – the umbo moved medially, but the lateral process approximately 4 mm more superior did not move.

Umbo displacements are shown for TT and St pulls (solid and dotted lines, respectively) in all three temporal bones in Fig. 10. In general, TT pulls produced greater umbo displacements (up to 0.2 mm for a 300 mN force) than St pulls (up to about 0.1 mm for a 300 mN force). Importantly, TT pulls caused *medial* umbo displacements, while St pulls typically caused *lateral* umbo displacements. These results, which are consistent with previous studies in animals (Loeb, 1964; Møller, 1963) and human temporal bones, imply that the TT and St muscles may act in opposition (Hüttenbrink, 1988b, 1989; Love and Stream, 1978).

4. Discussion

4.1. The effect of TT-muscle pulls on TM shape

It has been hypothesized that ME sound transmission is affected by the shape of the TM (through geometric nonlinearities) and its material properties (e.g., Fay et al., 2006; Motallebzadeh and Puria, 2022). Fig. 9 shows that TT-muscle pulls affected the conical shape of the TM. Using computational models for the cat TM, Fay et al., (2006) showed that the TM cone depth had a substantial effect on sound transmission. In that paper, they predicted that an increase in cone depth by a factor of 2, such that the inner conical region was larger and the outer toroidal region smaller, decreased the ME gain slightly at low frequencies and increased it slightly at high frequencies. On the other hand, decreasing the cone depth by a factor of 10, such that it was nearly flat, dramatically decreased the ME gain above about 1 kHz by up to 25 dB. Their conclusion was that this flatter eardrum better matched the impedance of air but lacked the stiffness needed to drive the higher-impedance umbo. With the deeper cone, the TM stiffness increased, which they concluded worsened the impedance match and decreased sound transmission at low frequencies.

Fig. 9D–E shows that the inner cone region of the human TM increased in depth while the curvature of the outer toroidal region decreased in depth due to a 380 mN TT-muscle pull, such that the entire TM became more cone-like than before pulling. This is analogous to the 2 × deeper TM cone case in the model of the cat TM in Fay et al., (2006). Fig. 4A shows that a 380 mN TT pull that produced a ~10% increase in TM cone depth caused a 12 dB reduction in umbo velocity below about 1 kHz that is significantly

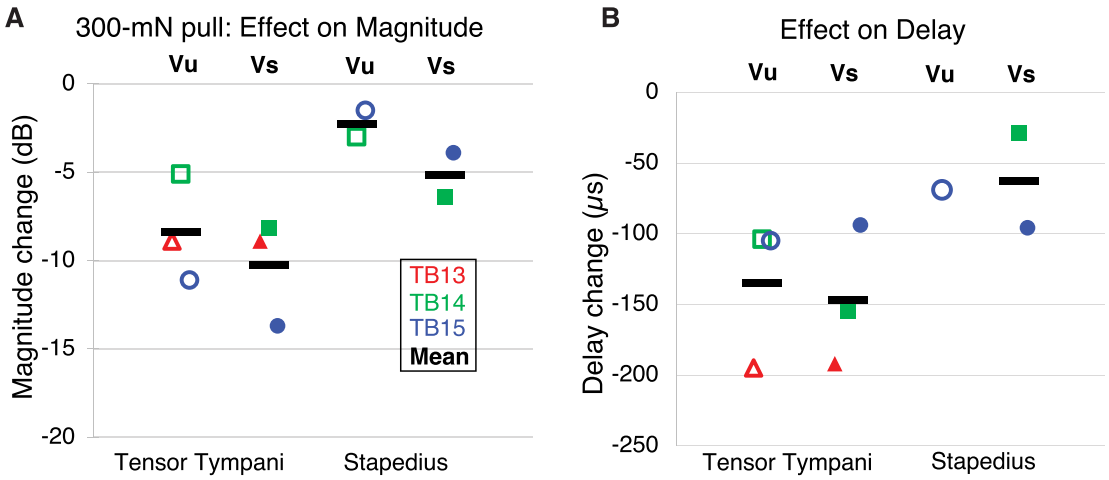

Fig. 11. Comparison and summary of the effects of a 300 mN muscle pull on low-frequency changes in velocity magnitude (**A**) and group delay (**B**) in all temporal bones: TB13: red triangles; TB14: green squares; TB15: blue circles; $\mathbf{V_U}$: open symbols; $\mathbf{V_S}$: filled symbols. TB13 $\mathbf{V_S}$ data and TB14 $\mathbf{V_U}$ delay with St pulls are omitted as described earlier.

greater than the 6 dB reduction predicted in the cat TM model for a much larger increase in cone depth. This result suggests that TT pulls had a much greater effect on sound transmission from changing the stiffness of the TM and ossicular chain than from changing the TM geometry.

We observed a difference in the umbo position depending on whether the TT or St muscle was pulled (Fig. 10). TT pulls caused the umbo to move medially, while St pulls caused the umbo to move laterally, in two temporal bones, by a roughly equal amount. This result has been seen previously (e.g., Hüttenbrink, 1989; Love and Stream, 1978), and it has been suggested that lateral umbo displacement by St pulls is robust except in cases of adhesions between the malleus and incus (Hüttenbrink, 1989). Though TT and St pulls moved the umbo in opposite directions, they had similar effects on ME sound transmission.

4.2. Summary of ME-muscle effects on V_U and V_S velocities

The different effects of increasing TT and St pulls on low-frequency $\mathbf{V_U}$ and $\mathbf{V_S}$ magnitudes shown in Fig. 8A and B are comparable to the effects of different TT and St pulls on tympanometric compliance in human temporal bones (Aron et al., 2015): Both show a steep reduction at low pull levels that becomes more shallow (greater additional force to produce additional change) for higher pulls.

To summarize the effects of TT and St pulls on low-frequency $\mathbf{V_U}$ and $\mathbf{V_S}$ magnitudes and group delays, we evaluated these at a pull level near 300 mN, as shown in Fig. 11. The following trends are observed:

(1) The effects of TT pulls on $|\mathbf{V_U}|$ and $|\mathbf{V_S}|$ (about 10 dB on average) were greater than the effects of St pulls (up to 5 dB on average). Though the size of this effect varied between temporal bones, the effect was consistent.
(2) The effects of TT or St pulls were greater on $|\mathbf{V_S}|$ than on $|\mathbf{V_U}|$.
(3) The effects of TT pulls on $\mathbf{V_U}$ and $\mathbf{V_S}$ group delays (140 μs on average) were generally about 2 × greater than the effects of St pulls (70 μs on average).
(4) TT pulls had similar effects on $\mathbf{V_U}$ and $\mathbf{V_S}$ group delays.
(5) St pulls had similar effects on $\mathbf{V_U}$ and $\mathbf{V_S}$ group delays.

The general trends were seen in each temporal bone, and TB15 provides a good example of these trends. The differences between TT and St pull effects were robust and seen in all measurements.

4.3. The effects of ME-muscle pulls on ME sound transmission

How much of the muscle-pull reduction in $\mathbf{V_S}$ magnitude is due to a reduction of sound collected by the TM, and how much is due to a change within the ME? As can be seen in Fig. 4, the effect of TT pulls on low-frequency velocity magnitude in TB15 was larger for $\mathbf{V_S}$ than for $\mathbf{V_U}$. This result implies that, below about 1.5 kHz, TT pulls not only reduce the amount of sound collected by the TM but also affect sound transmission through the ME. This is consistent with the finding that TT pulls also displace the stapes statically (Hüttenbrink, 1989). Between about 1.5 and 2.5 kHz, the effects of TT pulls on $|\mathbf{V_U}|$ and $|\mathbf{V_S}|$ were nearly identical, which implies that all the reduction in $|\mathbf{V_S}|$ in this frequency range is due to TT-muscle effects at the umbo. At higher frequencies, the effects of TT pulls were larger on $|\mathbf{V_S}|$ in narrow frequency ranges. Similar results were observed at low frequencies with TT pulls in TB13 and TB14 – see Fig. 8A.

The effects of St pulls on low-frequency velocity magnitudes in TB15 followed this same pattern (Fig. 6): larger effects on $|\mathbf{V_S}|$ than on $|\mathbf{V_U}|$. For St pulls, this result is not surprising: the point of action of the stapedius tendon is near the stapes head, and the flexibility of the incudomalleolar joint (Willi et al., 2002) and incudostapedial joint (Mason, 2013) would be expected to isolate $\mathbf{V_U}$ from effects at the stapes, as has been demonstrated for stapes fixation (Nakajima et al., 2005).

The effects of TT pulls on low-frequency group delay were similar for $\mathbf{V_U}$ and $\mathbf{V_S}$ (Fig. 8C). For St pulls, we have delay-change data for both $\mathbf{V_U}$ and $\mathbf{V_S}$ only in TB15, but in that bone the differences in the effects on group delays between $\mathbf{V_U}$ and $\mathbf{V_S}$ were small.

4.4. Non-acoustic activation of the TT muscle

The effects of TT-muscle pulls that we observed on $\mathbf{V_U}$ and $\mathbf{V_S}$ are consistent with other observations of non-acoustic TT pulls or activity. Some people can contract their TT muscles voluntarily, and such contractions cause a visible displacement of the TM (Bance et al., 2013). Frequently these people report a perception of a low-frequency rumbling sound during these TT-muscle contractions (Aron et al., 2015; Bance et al., 2013; Fournier et al., 2022), and changes in tympanometric measures during TT-muscle contraction were similar to those observed in human cadaveric temporal bones when the TT was pulled (Aron et al., 2015). We observed that a sinusoidally modulated TT pull in a temporal bone produced

a detectable sound at the same frequency in the ear canal (not shown).

4.5. Implications of ME-transmission modulation: a possible role of ME muscles in sound localization?

At low frequencies, humans localize sound in the horizontal plane by detecting the interaural time difference (ITD), performed on a cycle-by-cycle basis, by comparing the arrival times of the phase of sound at the two ears. At frequencies above 1–2 kHz, humans rely more on the interaural level difference (ILD), as the ILD cue becomes more robust and the phase locking of auditory-nerve activity to incoming sound is less reliable; but when both cues are present, the ITD is the dominant cue (e.g., Wightman and Kistler, 1992). Since ME-muscle pulls can change ME transmission magnitude and delay (Fig. 8), the muscles could affect sound localization. For instance, the ∼150 μs decrease in $\mathbf{V_S}$ delay caused by a unilateral 300 mN TT pull corresponds to the interaural time delay of a sound at ±15° azimuth (Kuhn, 1977). The importance of ME muscles for sound localization is unknown.

While other mammals can move their pinnae to better localize sounds, the overt reflexive control of the pinnae has been lost in nearly all humans (Hackley, 2015). Control of the TM and low-frequency delay by the ME muscles may provide an alternative to pinna control for sound localization. A recent study in which human subjects performed eye saccades (varied their gaze direction without moving their heads, by changing their eye orientations in their orbits) showed that horizontal saccadic eye motions cause bilateral and opposite changes in eye-movement-related eardrum oscillations (EMREOs) that produced ear-canal pressures that were hypothesized to be produced by the TM being moved by the ME muscles or due to otoacoustic emissions (Gruters et al., 2018). In preliminary experiments, we found that a quick step-pull on the TT muscle caused changes in ear-canal sound pressure (not shown) on the same time scale as those measured by Gruters et al., (2018) with eye saccades. ME-muscle-induced changes in ME transmission delay may provide a way of mechanically changing ITD cues to help the brain perform sound localization, perhaps by helping to align ocular-centered visual and head-centered auditory representations of the spatial environment.

For ME-muscle activity to produce antisymmetric TM movement between the two ears and generate ITDs and ILDs, ME muscles would need to be activated unilaterally and/or there would need to be a tonic level of ME-muscle activity that could be modulated, such that a relaxation of ME muscles could produce the opposite effect to additional contraction. The result in Fig. 10 (also seen by others), that TT and St pulls move the TM in opposite directions, could explain the Gruters et al., (2018) results of roughly equal and opposite ear-canal pressure changes in the two ears as ipsilateral contraction of the TT muscle and contralateral contraction of the St muscle in conjunction with eye movements. The larger effects of the TT muscle vs. St muscle on $\mathbf{V_S}$ delay and magnitude would still produce an ITD and ILD even with such simultaneous contractions of each muscle.

The Gruters et al., (2018) results could also be explained by a tonic level of ME-muscle activity that is modulated in response to certain stimuli. Recent studies suggest that tonic TT-muscle activity is possible and implicate tonic TT-muscle activity in a cluster of symptoms (Aron et al., 2015) that has been named Tonic Tensor Tympani Syndrome (e.g., Fournier et al., 2022). Off-axis sound or eye movements (Gruters et al., 2018; Tasko et al., 2022) or perhaps other stimuli (as described in Wightman and Kistler, 1992) could increase TT-muscle contraction in the ipsilateral ear and reduce it in the contralateral ear. Such an asymmetric pattern of ME-muscle activity would decrease delay in the ipsilateral ear and perhaps increase delay in the contralateral ear, thus enhancing the ITD.

We have shown that ME-muscle pulls not only can produce an ITD but can generate an ILD at low frequencies when no ILD is produced by head acoustics. For instance, the 300 mN TT pull that caused a ∼150 μs decrease in $\mathbf{V_S}$ delay also caused a ∼10 dB reduction in sound-transmission magnitude. An ILD of this level would be produced at a 15° azimuth only at frequencies above 10 kHz (Shaw, 1974). The antisymmetric TT modulation described above would produce a low-frequency ILD cue opposite to the ITD cue, but perhaps ILDs are not used for localization at low frequencies (Wightman and Kistler, 1992).

A potential complication to this argument is that most bilateral muscles involved in reflexes tend to be activated bilaterally. From what is known of ME-muscle reflexes, the stapedius reflex in cat is “grossly asymmetric” between ipsilateral and contralateral (McCue and Guinan, 1994), and there is doubt as to whether a contralateral TT-muscle reflex exists at all (e.g., Jones et al., 2008). It is also possible the ME-muscle activity in response to eye movements is fundamentally different than that associated with ME reflexes.

4.6. Sound and vision localization-acuity feedback

It is known that visual acuity is correlated with auditory acuity (measured as a minimum detectible angle). Animals that have good auditory acuity (e.g., 1° for human and 5° for cat) also have good visual acuity, while animals that have poor auditory acuity (e.g., 33° for mice and 28° for gerbil) also have poor visual acuity (Heffner and Heffner, 1992; Heffner et al., 2010). Thus, a narrow field of best vision is associated with better sound localization. This observation led to the notion that the primary purpose of sound localization in mammals is to direct an animal’s best visual field to the location of the sound source for further analysis (Heffner and Heffner, 1992).

When an ecologically important event occurs in the auditory–visual space, the representations of the two events are mapped onto the brain. We hypothesize that if the representations of visual and auditory events in the brain are misaligned, an error signal is produced which then sends signals through descending pathways to the ME muscles to reduce the error. We further hypothesize that this error minimization is in the form of adjusting interaural delays at the low frequencies. This error minimization may not necessarily be important for sound localization itself but for providing a real-time feedback signal between auditory and visual fields to inform the central mechanisms when the two coincide.

An example of when visual and auditory representations can become misaligned is when humans perform saccades in both horizontal and vertical directions. It has been shown that these saccades produce EMREOs that result in ear-canal pressures that parametrically capture the horizontal and vertical direction of the saccades, and thus eye-movement information is present at the eardrum (Lovich et al., 2022). The underlying mechanism behind this novel observation is yet to be determined. We interpret these EMREO recordings to be the signature of an error signal that is present at the very first stage of sound-to-neural coding and likely is present in higher centers. Ultimately, visual and auditory fields undergo spatial transformations that result in a co-aligned percept, and some of the circuitry for this is now being worked out (Caruso et al., 2021).

5. Summary

We examined the effects of graded TT- and St-muscle pulls, in physiologically reasonable ranges, on $\mathbf{V_U}$ and $\mathbf{V_S}$ magnitudes and phases. We found that, at low frequencies (below about 1–1.5 kHz):

(1) The effects of each ME muscle increased generally monotonically with increasing pull.

(2) The incremental effect of each ME-muscle pull decreased as pull increased.
(3) The effect of each ME muscle at low frequencies was to reduce ossicular-velocity magnitudes and increase ossicular-velocity phases relative to ear-canal sound pressure.
(4) The effect of each muscle on low-frequency phase was linear with frequency, consistent with a reduction of group delay.
(5) The effect of each ME muscle was relatively greater on $|\mathbf{V_S}|$ than on $|\mathbf{V_U}|$.
(6) The effects of TT-muscle pulls on $\mathbf{V_U}$ and $\mathbf{V_S}$ magnitudes and group delays were nearly twice as much as the effects of St-muscle pulls.
(7) For each ME muscle, similar pulls produced similar effects on $\mathbf{V_U}$ and $\mathbf{V_S}$ group delays.
(8) Modulation of $\mathbf{V_S}$ group delay by ME-muscle action could generate an interaural time delay that could aid in sound localization and/or alignment of auditory and visual fields.

These measurements of TT- and St-muscle effects on ME sound transmission and low-frequency delay provide an intriguing glimpse into possible previously unknown roles and functions of the ME muscles. Further research could elucidate functional differences in TT- and St-muscle activation, provide methods to distinguish between their effects, and explore the effects and implications of simultaneous activation of both muscles.

Funding source

This work was supported by the Amelia Peabody Charitable Foundation (to Sunil Puria).

Author statement

The contributions of each author are briefly described below:

- All authors conceived and designed the project, performed the experiments, analyzed the data, and co-wrote the manuscript.
- Nam Hyun Cho developed the VibOCT software, and plotted data.
- Michael E. Ravicz set up the acoustic equipment and developed the force sensor and software.
- Sunil Puria supervised the project.

Supplementary materials

None.

Declaration of Competing Interest

The authors have no competing interests to declare.

Data availability

Data will be made available on request.

Acknowledgements

The authors thank Diane Jones and Anbuselvan Dharmarajan of the Otopathology Lab at Massachusetts Eye and Ear and Xiying Guan (now at Wayne State University) for help in procuring and preparing temporal bones; Haobing Wang for enhancements to the EPL anatomical viewer; Kevin N. O'Connor for modifications to SyncAv software to run the experiments and for data analysis scripts (SyncAv Toolbox) and editing assistance; Inge Knudsen for help with references; and the staff of the Eaton-Peabody Laboratories. We also thank reviewers Matthew Mason, Jennifer M. Groh, and Cynthia D. King as well as an anonymous reviewer for their detailed comments and helpful suggestions that have resulted in a significantly improved manuscript.

References

Amoako-Tuffour, Y., Garland, P., Bance, M., 2016. Interpretation of sonotubometric data based on phase-shift detection. J. Otolaryngol. Head. Neck Surg. 45 (1), 37. doi:10.1186/s40463-016-0151-5.
Aron, M., Floyd, D., Bance, M., 2015. Voluntary eardrum movement: a marker for tensor tympani contraction? Otol. Neurotol. 36 (2), 373–381. doi:10.1097/MAO.0000000000000382.
Bance, M., Makki, F.M., Garland, P., Alian, W.A., van Wijhe, R.G., Savage, J., 2013. Effects of tensor tympani muscle contraction on the middle ear and markers of a contracted muscle. Laryngoscope 123 (4), 1021–1027. doi:10.1002/lary.23711.
Blevins, C.E., 1968. Motor units in the stapedius muscle. Arch. Otolaryngol. 87 (3), 249–254. doi:10.1001/archotol.1968.00760060251007.
Borg, E., Counter, S.A., Rosler, G., 1984. Theories of middle-ear muscle function. In: Silman, S. (Ed.), The Acoustic Reflex: Basic Principles and Clinical Applications. Academic Press, New York, pp. 63–99.
Bosatra, A., Russolo, M., Semeraro, A., 1975. Tympanic muscle reflex elicited by electric stimulation of the tongue in normal and pathological subjects. Acta Otolaryngol. 79 (5–6), 334–338.
Caruso, V.C., Pages, D.S., Sommer, M.A., Groh, J.M., 2021. Compensating for a shifting world: evolving reference frames of visual and auditory signals across three multimodal brain areas. J. Neurophysiol. 126 (1), 82–94. doi:10.1152/jn.00385.2020.
Cho, N.H., Puria, S., 2022. Cochlear motion across the reticular lamina implies that it is not a stiff plate. Sci. Rep. 12 (1), 18715. doi:10.1038/s41598-022-23525-x.
Cho, N.H., Wang, H., Puria, S., 2022. Cochlear fluid spaces and structures of the gerbil high-frequency region measured using optical coherence tomography (OCT). J. Assoc. Res. Otolaryngol. 23 (2), 195–211. doi:10.1007/s10162-022-00836-4.
Fay, J.P., Puria, S., Steele, C.R., 2006. The discordant eardrum. Proc. Natl. Acad. Sci. U. S. A. 103 (52), 19743–19748. doi:10.1073/pnas.0603898104.
Fournier, P., Paquette, S., Paleressompoulle, D., Paolino, F., Deveze, A., Norena, A., 2022. Contraction of the stapedius and tensor tympani muscles explored by tympanometry and pressure measurement in the external auditory canal. Hear. Res. 420, 108509. doi:10.1016/j.heares.2022.108509.
Funnell, W.R., Laszlo, C.A., 1978. Modeling of the cat eardrum as a thin shell using the finite-element method. J. Acoust. Soc. Am. 63 (5), 1461–1467.
Gallagher, L., Diop, M., Olson, E.S., 2021. Time-domain and frequency-domain effects of tensor tympani contraction on middle ear sound transmission in gerbil. Hear. Res. 405, 108231. doi:10.1016/j.heares.2021.108231.
Gelfand, S.A., 1998. Hearing: an Introduction to Psychological and Physiological Acoustics, 3rd ed. Marcel Dekker, New York.
Gottlieb, P.K., Vaisbuch, Y., Puria, S., 2018. Human ossicular-joint flexibility transforms the peak amplitude and width of impulsive acoustic stimuli. J. Acoust. Soc. Am. 143 (6), 3418–3433. doi:10.1121/1.5039845.
Gruters, K.G., Murphy, D.L.K., Jenson, C.D., Smith, D.W., Shera, C.A., Groh, J.M., 2018. The eardrums move when the eyes move: a multisensory effect on the mechanics of hearing. Proc. Natl. Acad. Sci. U. S. A. 115 (6), E1309–E1318. doi:10.1073/pnas.1717948115.
Hackley, S.A., 2015. Evidence for a vestigial pinna-orienting system in humans. Psychophysiology 52 (10), 1263–1270. doi:10.1111/psyp.12501.
Heffner, R.S., Heffner, H.E., 1992. Visual factors in sound localization in mammals. J. Comp. Neurol. 317 (3), 219–232. doi:10.1002/cne.903170302.
Heffner, R.S., Koay, G., Heffner, H.E., 2010. Use of binaural cues for sound localization in large and small non-echolocating bats: eidolon helvum and Cynopterus brachyotis. J. Acoust. Soc. Am. 127 (6), 3837–3845. doi:10.1121/1.3372717.
Howell, P., 1984. Are two muscles needed for the normal functioning of the mammalian middle ear? Acta Otolaryngol. 98 (3–4), 204–207.
Hüttenbrink, K.B., 1988a. [The fixation theory of middle ear muscle function]. Laryngol. Rhinol. Otol. (Stuttg). 67 (8), 404–411.
Hüttenbrink, K.B., 1988b. The mechanics of the middle-ear at static air pressures: the role of the ossicular joints, the function of the middle-ear muscles and the behaviour of stapedial prostheses. Acta Otolaryngol. Suppl. 451, 1–35.
Hüttenbrink, K.B., 1989. [The functional significance of the suspending ligaments of the ear ossicle chain]. Laryngorhinootologie 68 (3), 146–151.
Hüttenbrink, K.B., 1992. [The mechanics and function of the middle ear. Part 1: the ossicular chain and middle ear muscles]. Laryngorhinootologie 71 (11), 545–551.
Jones, S.E., Mason, M.J., Sunkaraneni, V.S., Baguley, D.M., 2008. The effect of auditory stimulation on the tensor tympani in patients following stapedectomy. Acta Otolaryngol. 128 (3), 250–254. doi:10.1080/00016480701509925.
Khaleghi, M., Cheng, J.T., Furlong, C., Rosowski, J.J., 2016. In-plane and out-of-plane motions of the human tympanic membrane. J. Acoust. Soc. Am. 139 (1), 104–117. doi:10.1121/1.4935386.
Kuhn, G.F., 1977. Model for the interaural time differences in the azimuthal plane. J. Acoust. Soc. Am. 62 (1), 157–167. doi:10.1121/1.381498.
Lauxmann, M., Eiber, A., Heckeler, C., Ihrle, S., Chatzimichalis, M., Huber, A., Sim, J.H., 2012. In-plane motions of the stapes in human ears. J. Acoust. Soc. Am. 132 (5), 3280–3291. doi:10.1121/1.4756925.
Loeb, M., 1964. Psychophysical correlates of intratympanic reflex action. Psychol. Bull. 61, 140–152. doi:10.1037/h0047660.
Love Jr, J.T., Stream, R.W., 1978. The biphasic acoustic reflex: a new perspective. Laryngoscope 88 (2), 298–313. doi:10.1288/00005537-197802000-00012, Pt 1.
Lovich, S.N., King, C.D., Murphy, D.L., Landrum, R., Shera, C.A., Groh, J.M., 2022. Parametric Information about Eye Movements is Sent to the Ears. bioRxiv 2022.2011.2027.518089 doi:10.1101/2022.11.27.518089.
Manley, G.A., 2010. The origin and evolution of high-frequency hearing in (most) mammals. Hear. Res. 270 (1–2), 2–3. doi:10.1016/j.heares.2010.08.010.

Mansour, S., Magnan, J., Haidar, H., Nicolas, K., Louryan, S.p., 2013. Comprehensive and Clinical Anatomy of the Middle Ear. Springer, Heidelberg.
Marquet, J., 1981. The incudo-malleal joint. J. Laryngol. Otol. 95 (6), 543–565.
Mason, M.J., 2013. Of mice, moles and guinea pigs: functional morphology of the middle ear in living mammals. Hear. Res. 301, 4–18. doi:10.1016/j.heares.2012.10.004.
Mason, M.J., Farr, M.R., 2013. Flexibility within the middle ears of vertebrates. J. Laryngol. Otol. 127 (1), 2–14. doi:10.1017/S0022215112002496.
McCue, M.P., Guinan Jr, J.J., 1994. Acoustically responsive fibers in the vestibular nerve of the cat. J. Neurosci. 14 (10), 6058–6070.
Møller, A.R., 1963. Transfer function of the middle ear. J. Acoust. Soc. Am. 35 (10), 1526–1534. doi:10.1121/1.1918742.
Motallebzadeh, H., Puria, S., 2022. Stimulus-frequency otoacoustic emissions and middle-ear pressure gains in a computational mouse model. J. Acoust. Soc. Am. in press.
Nakajima, H.H., Ravicz, M.E., Merchant, S.N., Peake, W.T., Rosowski, J.J., 2005. Experimental ossicular fixations and the middle ear's response to sound: evidence for a flexible ossicular chain. Hear. Res. 204 (1–2), 60–77.
Nuttall, A.L., 1974. Tympanic muscle effects on middle-ear transfer characteristic. J. Acoust. Soc. Am. 56 (4), 1239–1247.
O'Connor, K.N., Puria, S., 2006. Middle ear cavity and ear canal pressure-driven stapes velocity responses in human cadaveric temporal bones. J. Acoust. Soc. Am. 120 (3), 1517–1528.
Olson, E.S., 1998. Observing middle and inner ear mechanics with novel intracochlear pressure sensors. J. Acoust. Soc. Am. 103, 3445–3463.
Pang, X.D., Guinan Jr, J.J., 1997. Effects of stapedius-muscle contractions on the masking of auditory-nerve responses. J. Acoust. Soc. Am. 102 (6), 3576–3586.
Pang, X.D., Peake, W.T., 1986. How do contractions of the stapedius muscle alter the acoustic properties of the middle ear? In: Allen, J.B., Hall, J.L., Hubbard, A., Neely, S.T., Tubis, A. (Eds.), Peripheral Auditory Mechanisms. Springer-Verlag, Boston, MA.
Parent, P., Allen, J.B., 2010. Time-domain "wave" model of the human tympanic membrane. Hear. Res. 263 (1–2), 152–167. doi:10.1016/j.heares.2009.12.015.
Puria, S., 2020. Middle-Ear Biomechanics: Smooth Sailing, Acoustics Today. AIP, NY.
Puria, S., Allen, J.B., 1998. Measurements and model of the cat middle ear: evidence of tympanic membrane acoustic delay. J. Acoust. Soc. Am. 104 (6), 3463–3481.
Rosowski, J.J., 1994. Outer and middle ears. In: Fay, R.R., Popper, A.N. (Eds.), Comparative hearing. Mammals. Springer-Verlag, New York, p. 260 xi.
Rosowski, J.J., Chien, W., Ravicz, M.E., Merchant, S.N., 2007. Testing a method for quantifying the output of implantable middle ear hearing devices. Audiol. Neurootol. 12 (4), 265–276. doi:10.1159/000101474.
Shaw, E.A., 1974. Transformation of sound pressure level from the free field to the eardrum in the horizontal plane. J. Acoust. Soc. Am. 56 (6), 1848–1861.
Sim, J.H., Steele, C.R., Puria, S., 2007. Calculation of inertia properties of the malleus-incus complex using micro-CT imaging. J. Mech. Mater. Struct. 2 (8), 1515–1524.
Tasko, S.M., Deiters, K.K., Flamme, G.A., Smith, M.V., Murphy, W.J., Jones, H.G., Greene, N.T., Ahroon, W.A., 2022. Effects of unilateral eye closure on middle ear muscle contractions. Hear. Res. 424, 108594. doi:10.1016/j.heares.2022.108594.
Teig, E., 1972a. Force and contraction velocity of the middle ear muscles in the cat and the rabbit. Acta Physiol. Scand. 84 (1), 1–10.
Teig, E., 1972b. Tension and contraction time of motor units of the middle ear muscles in the cat. Acta Physiol. Scand. 84 (1), 11–21.
Tucker, A.S., 2017. Major evolutionary transitions and innovations: the tympanic middle ear. Philos. Trans. R. Soc. Lond. B. Biol. Sci. 372 (1713). doi:10.1098/rstb.2015.0483.
Van der Jeught, S., Dirckx, J.J., Aerts, J.R., Bradu, A., Podoleanu, A.G., Buytaert, J.A., 2013. Full-field thickness distribution of human tympanic membrane obtained with optical coherence tomography. J. Assoc. Res. Otolaryngol. 14 (4), 483–494. doi:10.1007/s10162-013-0394-z.
Wang, H., Northrop, C., Burgess, B., Liberman, M.C., Merchant, S.N., 2006. Three-dimensional virtual model of the human temporal bone: a stand-alone, downloadable teaching tool. Otol. Neurotol. Off. Publ. Am. Otol. Soc. Am. Neurotol. Soc. Eur. Acad. Otol. Neurotol. 27 (4), 452–457. doi:10.1097/01.mao.0000188353.97795.c5.
Wickens, B., Floyd, D., Bance, M., 2017. Audiometric findings with voluntary tensor tympani contraction. J. Otolaryngol. Head Neck Surg. 46 (1), 2. doi:10.1186/s40463-016-0182-y.
Wightman, F.L., Kistler, D.J., 1992. The dominant role of low-frequency interaural time differences in sound localization. J. Acoust. Soc. Am. 91 (3), 1648–1661. doi:10.1121/1.402445.
Willi, U.B., Ferrazzini, M.A., Huber, A.M., 2002. The incudo-malleolar joint and sound transmission losses. Hear. Res. 174 (1–2), 32–44.